

**DOPPLER-BROADENED SPECTRAL EMISSION  
FROM THE TURBULENTLY HEATED PLASMA OF BURNOUT V \***

I. Alexeff, G. E. Guest, J. R. McNally, Jr., R. V. Neidigh, and F. R. Scott†

Oak Ridge National Laboratory, Oak Ridge, Tennessee 37830

(Received 2 June 1969)

In an efficient ion heating mode recently discovered in the Burnout-V turbulent-heating experiment, the line profiles of emission spectra exhibit three noteworthy features: (1) a marked Doppler broadening (full width at half-maximum  $\approx 10 \text{ \AA}$ ) of the Balmer lines, (2) a "red"/"blue" asymmetry dependent on the geometry of the plasma container, and (3) non-Gaussian line shapes near the central wavelengths.

The turbulent-heating experiment, Burnout V<sup>1</sup> (dc, 50-kG mirrors, axial electron beam), has an average deuteron energy density that appears to increase exponentially with beam power through three separately identifiable and tractable plasma modes. In the most effective deuteron heating mode (third mode) typical spectral distributions for  $D_\alpha$ ,  $D_\beta$ , and  $D_\gamma$  taken perpendicular to the magnetic field, together with a sketch of the method of observation, are shown in Fig. 1.

Because the maximum plasma density is  $(3-5) \times 10^{13} \text{ cm}^{-3}$ , Stark broadening due to ionic fields is negligible ( $<1 \text{ \AA}$ ) compared with the observed linewidth of  $10 \text{ \AA}$  in the broad part of the line-intensity distribution. Moreover, the linewidths of the three lines observed ( $D_\alpha$ ,  $D_\beta$ , and  $D_\gamma$ ) are roughly proportional to their central wavelengths

as expected for Doppler broadening. We therefore interpret the broad line profiles as arising from the thermal motion of the emitting neutral particles. On this basis we distinguish between emission from "cold" so-called Franck-Condon atoms (2-10 eV), excited in molecular dissociation and by inelastic electron collisions, and emission from fast atoms where average energy is between 1 and 2 keV based on the Doppler widths. The former contribute only to the central spike of the line profile, whose width ( $\sim 2 \text{ \AA}$ ) is approximately equal to the instrumental width ( $100\text{-}\mu$  slits), whereas the latter give rise to a nearly Gaussian profile for  $|\Delta\lambda| \geq 5 \text{ \AA}$ ; this fits a Doppler distribution of velocities.

As shown in Fig. 1, the line profiles are not symmetric about the central wavelength; rather, the blue wing ( $\Delta\lambda < 0$ ) is more intense than the red ( $\Delta\lambda > 0$ ). Since this asymmetry is maintained for all sectors through the plasma volume (Fig. 2), mass rotation is not a plausible explanation. To explain this, we conjecture that the asymmetry results from a finite rate of feed into the upper level of the observed transition. That is, highly excited energetic neutral atoms arising from charge exchange of fast ions on slow neutrals move radially outward at sufficient speed that an appreciable number strike the wall and are lost before emitting radiation. Thus, since the distance from the plasma to the front of the machine ( $b$  in Fig. 1) is larger than the distance to the rear of the machine ( $a$  in Fig. 1), forward-moving atoms have more time to emit than rearward-moving atoms, and a therefore greater blue intensity results. Container geometry variations were effected by varying lengths  $a$  and  $b$  shown in the insert of Fig. 1. Experimentally, the relative blue/red intensity was found to be dependent on the geometrical ratio  $b/a$ ; symmetric line profiles result for  $b = a$ . Thus highly excited energetic neutral atoms arising from charge exchange of fast ions on slow neutrals move radially outward from the plasma core at sufficient

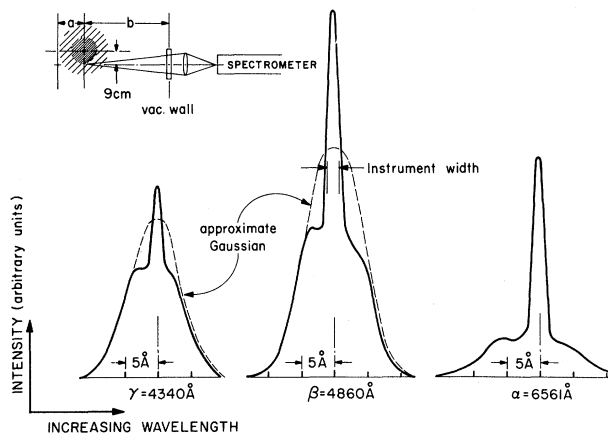


FIG. 1. Doppler broadened Balmer- $\alpha$ , - $\beta$ , and - $\gamma$  spectra. The asymmetry of the broadened lines is a plasma container effect. Longer transit time to the most distant wall (blue wing) permits greater population of  $n=4$  level because of delayed cascading. Abnormally low intensity at small  $\Delta\lambda$  is most likely due to small charge-exchange cross sections for low-energy deuterons on Franck-Condon neutrals and impurities. Slit widths were  $100 \mu$  giving the instrument width shown. The spectrometer observed a sector through the plasma at approximately 9 cm from the axis.

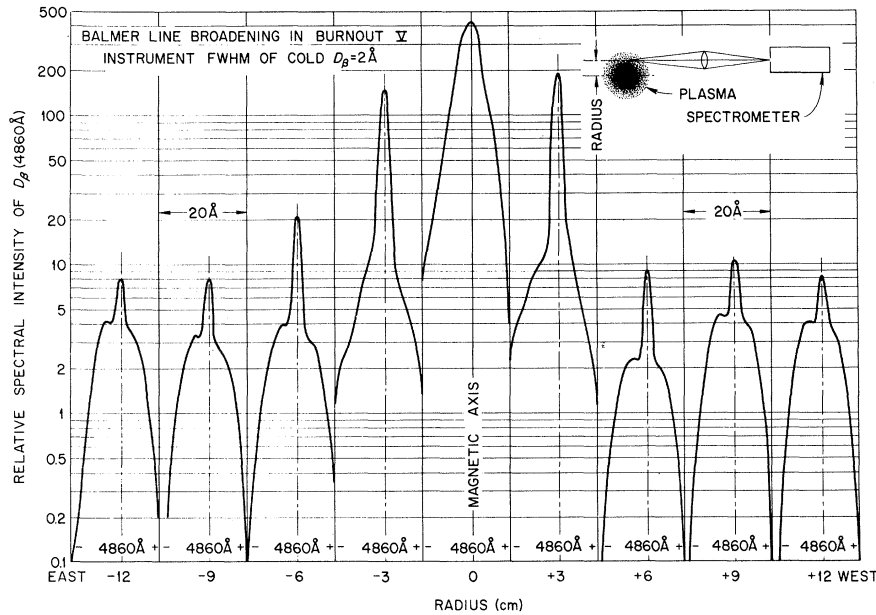
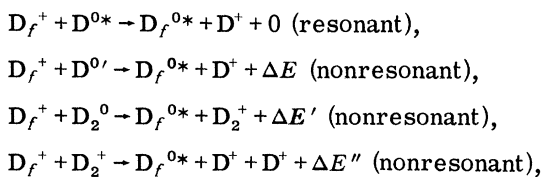


FIG. 2. Balmer- $\beta$  intensity for different plasma sectors. Maximum intensity is on the blue side of the Doppler-broadened line. The asymmetry is barely detectable in the sector through the axis.

speed to render their transit times to the observation point comparable with the time for cascading down to the upper level of the transition being observed ( $n=4$  for  $D_\beta$ ). Since this model suggests that the probability for emission is proportional to  $\exp(-\tau_{\text{cascade}}/\tau_{\text{transit}})$ , where  $\tau_{\text{transit}} = (\text{distance})/(\text{velocity})$  of neutral, and  $\tau_{\text{cascade}} \approx 10^{-6}$  sec according to Allen,<sup>2</sup> we seek confirmatory evidence through spectral observations at varying radii. As shown in Fig. 3, the spectrum "hardens" slightly as anticipated as the point of observation is increased from 0 to 9 cm because of the time-delay increase.

The non-Gaussian line shape near the central wavelength (excluding the central peak which arises from  $\sim 5$ -eV neutrals), illustrated in Fig. 1, admits no simple interpretation because of the many uncertainties in the charge-transfer processes relating the fast-ion particle distribution to the atomic-emission line shape. We expect the dominant charge-exchange reactions to be



where  $D_f^+$  represents fast deuterons,  $D^{0*}$  represents deuterium atoms, and  $\Delta E$  is the energy defect of the particular charge-exchange reaction.

The cross sections for the nonresonant reactions are known to decrease rapidly with decreasing energy and to have smaller cross sections than the resonant reactions.<sup>3</sup>

It is difficult to extract an ion-energy density

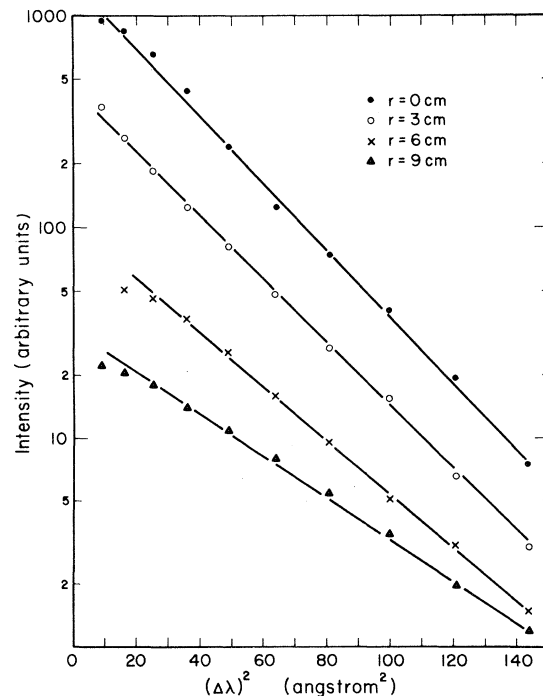


FIG. 3. Intensity  $I$  vs  $(\Delta\lambda)^2$  for blue wing at different radii. Note that radiation appears to harden with increased radius.

distribution from the spectral data presented. Indeed the most difficult problem here is that of appropriate unfolding of the line profile. However if we assume somewhat arbitrarily that the energetic excited atoms result mainly from resonant charge exchange on excited atomic neutrals, we can use the observed spectrum to estimate a distribution of fast ions within the plasma. The resulting average ion energy we find to be in rough agreement with that inferred from velocity analysis of escaping neutrals atoms (1-2 keV) as expected.

We wish to express our appreciation to B. S. Turner and J. G. Harris for their inventiveness and technical skill in the development of the ex-

periment.

---

\*Research sponsored by the U. S. Atomic Energy Commission under contract with the Union Carbide Corporation.

†Consultant, University of Tennessee, Knoxville, Tenn.

<sup>1</sup>I. Alexeff, W. D. Jones, and R. V. Neidigh, *Phys. Rev. Letters* **18**, 1109 (1967); R. V. Neidigh et al., in *Plasma Physics and Controlled Nuclear Fusion Research* (International Atomic Energy Agency, Vienna, Austria, 1969), Paper No. CN-24/L-2.

<sup>2</sup>C. W. Allen, *Astrophysical Quantities* (The Athlone Press, University of London, London, England, 1955), p. 63.

<sup>3</sup>H. S. W. Massey, *Rept. Progr. Phys.* **12**, 248 (1949).

---

### OSMOTIC PRESSURE OF DEGENERATE He<sup>3</sup>-He<sup>4</sup> MIXTURES\*

J. Landau, J. T. Tough, N. R. Brubaker, and D. O. Edwards  
 Department of Physics, Ohio State University, Columbus, Ohio 43210  
 (Received 16 June 1969)

The osmotic pressure of He<sup>3</sup>-He<sup>4</sup> mixtures has been measured down to 0.027°K. The results are used (a) to check the validity of the He<sup>3</sup>-He<sup>3</sup> effective interaction deduced from transport data using recent exact solutions of the Boltzmann transport equation, (b) to obtain the limiting solubility of He<sup>3</sup> in He<sup>4</sup> as a function of pressure, and (c) to demonstrate the metastability of supersaturated mixtures of He<sup>3</sup> in He<sup>4</sup> in the absence of a free surface.

Recently, exact solutions for the Boltzmann equation of a degenerate Fermi liquid have been worked out by Brooker and Sykes<sup>1</sup> and by Højgaard Jensen, Smith, and Wilkins.<sup>2</sup> The exact solutions have been employed by Ebner<sup>3</sup> to redetermine the Bardeen, Baym, and Pines<sup>4</sup> (BBP) He<sup>3</sup>-He<sup>3</sup> effective interaction from experimental data on the transport properties of helium mixtures. The static or thermodynamic properties of mixtures also depend on the interaction, and one can make an independent test of the theory by comparing thermodynamic data with the predictions of BBP calculated from transport data. Previous tests of this sort<sup>5-7</sup> in the degenerate region have been only semiquantitative or have needed extrapolation of the Fourier transform  $V(k)$  of the interaction to higher values of  $k$  than can be deduced from the transport data.

The osmotic pressure  $\pi$ , which can be thought of as the pressure of the He<sup>3</sup> quasiparticle gas, has a fairly large contribution from the effective interaction at 0°K and this is one reason why the present relatively precise measurements of  $\pi$  were undertaken. The experiments were performed at pressures  $P$  up to 20 atm so that, in

addition, we could determine how the solubility of He<sup>3</sup> in He<sup>4</sup> varied with pressure. This result, as well as the metastability of supersaturated mixtures observed in the experiments, has some relevance to the possibility of a pairing condensation at low temperatures<sup>4,8</sup> and will be useful for the design and analysis of other experiments on mixtures under pressure.

The experimental cell was maintained at temperatures from 0.027 to 0.65°K by a dilution refrigerator, and contained two chambers each with a capillary, one for adding He<sup>3</sup> and one for pressurizing the system with He<sup>4</sup>. The mixture chamber contained a cerium magnesium nitrate thermometer and communicated with the pure He<sup>4</sup> chamber through a superleak.<sup>9</sup> The differential pressure across the superleak, the osmotic pressure  $\pi$ , was measured with a specially designed diaphragm pressure gauge,<sup>10</sup> calibrated *in situ* against the earlier, absolute-osmotic-pressure measurements of Wilson, Edwards, and Tough<sup>11</sup> at 0.65°K.

Measurements obtained with the present apparatus at 0.32°K and He<sup>3</sup> mole fraction  $X = 1.5\%$  agree very well with the data of Wilson, Edwards,